The Relationship between the Madden–Julian Oscillation and Tropical Cyclone Rapid Intensification

SIM D. ABERSON AND J. KAPLAN

NOAA/AOML/Hurricane Research Division, Miami, Florida

(Manuscript received 8 October 2019, in final form 24 June 2020)

ABSTRACT

The relationship between the Madden–Julian oscillation (MJO) and tropical cyclone rapid intensification in the northern basins of the Western Hemisphere is examined. All rapid intensification events in the part of the Western Hemisphere north of the equator and the MJO phase and amplitude are compiled from 1974 to 2015. Rapid intensification events and the MJO tend to move in tandem with each other from west to east across the hemisphere, though rapid intensification appears most likely during a neutral MJO phase. The addition of this information to an operational statistical rapid intensification forecasting scheme does not significantly improve forecasts.

1. Introduction

The Madden–Julian oscillation (MJO) is a large-scale oscillation in the equatorial troposphere with a period generally between 30 and 50 days (Madden and Julian 1972). The oscillation appears to move eastward accompanied by fluctuations in the zonal wind, vertical motion, moisture, and convection. The change in zonal wind velocity modifies vertical wind shear, and these cumulative changes may alter tropical cyclone activity, especially cyclogenesis, globally (Liebmann et al. 1994; Leroy and Wheeler 2008; Camargo et al. 2009; Klotzbach 2010; Ventrice et al. 2011; Slade and Maloney 2013; Crosbie and Serra 2014; Klotzbach and Oliver 2015; Zhao and Li 2019). Despite the large number of studies on the relationship between the MJO and tropical cyclone activity, the only published work on the relationship between tropical cyclone rapid intensification [RI; herein defined as an increase to the maximum sustained wind speed of at least 30 kt ($1\,\mathrm{kt} \approx 0.51\,\mathrm{m\,s^{-1}}$) in 24 h (Kaplan and DeMaria 2003)] has been by Klotzbach (2012). They found that, in the Atlantic basin, RI is 4 times more likely during the active MJO phase than during the inactive phase, but did not explore whether the MJO can be useful in predictive schemes for RI. The current study is an effort to extend Klotzbach (2012) to the central and east Pacific, and to test whether the MJO may have predictive capability in current forecast schemes. Section 2 describes the data used, followed by initial results from binning of RI cases by MJO phase in section 3. Section 4 discusses a test of potential MJO predictors in a statistical RI forecast technique, and conclusions follow.

2. Data

The North Atlantic and northeast and north-central Pacific hurricane databases [i.e., the NHC "best track" hurricane database (HURDAT2; Landsea and Franklin 2013)] are used in the study. All RI events from 1974 to 2015 in the three basins are included in the study, including consecutive events; for example, if the intensity of a particular TC increased by 30 kt from 0000 UTC to 0000 UTC the next day, and also from 0600 UTC to 0600 UTC the next day, both events are counted. A total of 2657 such events occurred during the 42-yr period, with considerable interannual variability and a slight increase in the number of events in time (Fig. 1).

Wheeler and Hendon (2004) defined two real-time multivariate modes (RMM) of upper- and lower-level winds and outgoing longwave radiation and defined a two-dimensional phase space to quantify the MJO phase and amplitude.[1] The index removes the seasonal cycle

[1] Alternative indices such as the outgoing longwave radiation-based (OLR-based) MJO index (Kiladis et al. 2014) have been tested, and the results are not substantially different than those presented using the Wheeler–Hendon index.

Corresponding author: Sim D. Aberson, sim.aberson@noaa.gov

DOI: 10.1175/WAF-D-19-0209.1

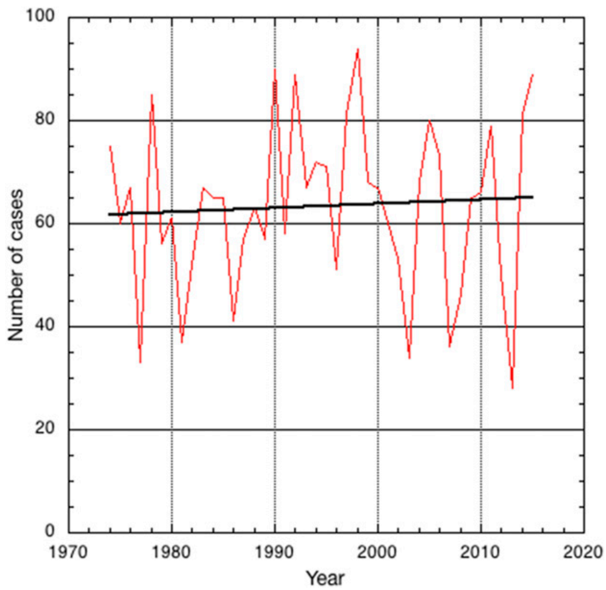

FIG. 1. Annual numbers of RI events in the Atlantic, east Pacific, and central Pacific basins (red); a linear fit to the data is shown by the thick black line.

and some low-frequency variability associated with El Niño–Southern Oscillation. They defined eight phases: in phase 1, the convection is enhanced over Africa and the western Indian Ocean. As the phase number increases, the region of enhanced convection moves eastward past the Australasian landmass (phase 5) and over the Pacific and Atlantic (phases 7 and 8, respectively). The index is available since 1974, except for the period from April to December 1978. All RMM1 and RMM2 values from 1 June 1974 to 31 December 2015 are shown in Fig. 2a. The values of both components are between −4 and +4; the averages of the two are −0.02 and −0.03, respectively, suggesting a mean neutral state.

3. Results

The longitude where each RI[2] event began is noted, and the events are binned into 20°-wide overlapping regions from 180° to 10°W in 10° increments. All RMM values and their means in the westernmost, middle, and easternmost bins are shown in Figs. 2b–d, respectively. The westernmost bin (Fig. 2b) is biased toward negative RMM1 values, whereas the easternmost bin (Fig. 2d) is biased toward positive values. The central region (Fig. 2c) contains mainly negative values of both RMM components.

[2] Higher intensification rates during the 24-h period have been tested, with similar results, though the numbers of cases in each bin are necessarily smaller than those reported here.

Figure 3 shows the mean RMM values of RI cases in each longitudinal bin and a polynomial fit to those values. The mean amplitudes are generally small (<0.5) and decrease from the central Pacific to the eastern Atlantic, much like the MJO amplitude tends to decrease through those regions. As the RI events occur farther eastward, the average phase moves from phase 8 counterclockwise to phase 4, in the same direction as that of the MJO. This suggests a relationship between the MJO phase and RI occurrence in each longitudinal band. Tropical cyclone genesis is known to be enhanced in the Atlantic when the convectively active phase is located over Africa and the western Indian Ocean (Camargo et al. 2009; Klotzbach 2010). However, the mean phase for RI cases lags the most convectively active phase such that RI is most likely to occur during the transition from convectively active to inactive phases.

The RMM values for all RI events that began within each longitude region are combined into two samples (one each for RMM1 and RMM2). Statistical significance of the differences of the means of each are tested individually using an unpaired t test, and the results are shown in Fig. 4. For example, for the 180°–160° bin, the sample means of either RMM1 or RMM2 are statistically different at the 99% confidence level or higher from those samples in all other longitude bins except the nearest one. In all, many adjacent bins are not statistically different from each other, but all bins more than 60° longitude from each other are significantly different at the 99% level. Though the sample sizes on the extrema are relatively small, the statistical tests suggest a <1% probability that the differences are not robust.

The reason for the lag between the convectively active MJO phase (when tropical cyclogenesis is most likely) and RI events is not clear. Most tropical cyclones undergoing RI, especially in the deep tropics, move westward while the MJO moves eastward; since tropical cyclones generally do not undergo RI immediately upon genesis, the few days between the two events allows the tropical cyclone and the MJO to move in opposite directions, possibly creating this phase lag. Alternatively, since the MJO has a strong signal with cyclogenesis, which is a necessary condition for RI, the only impact the MJO has on RI itself may be in creating the precursor tropical cyclones for RI to occur.

4. Test as a predictor in SHIPS-RII

To test whether information on the MJO could be used to improve statistical RI-forecast guidance, additional parameters related to RMM1 and RMM2 were

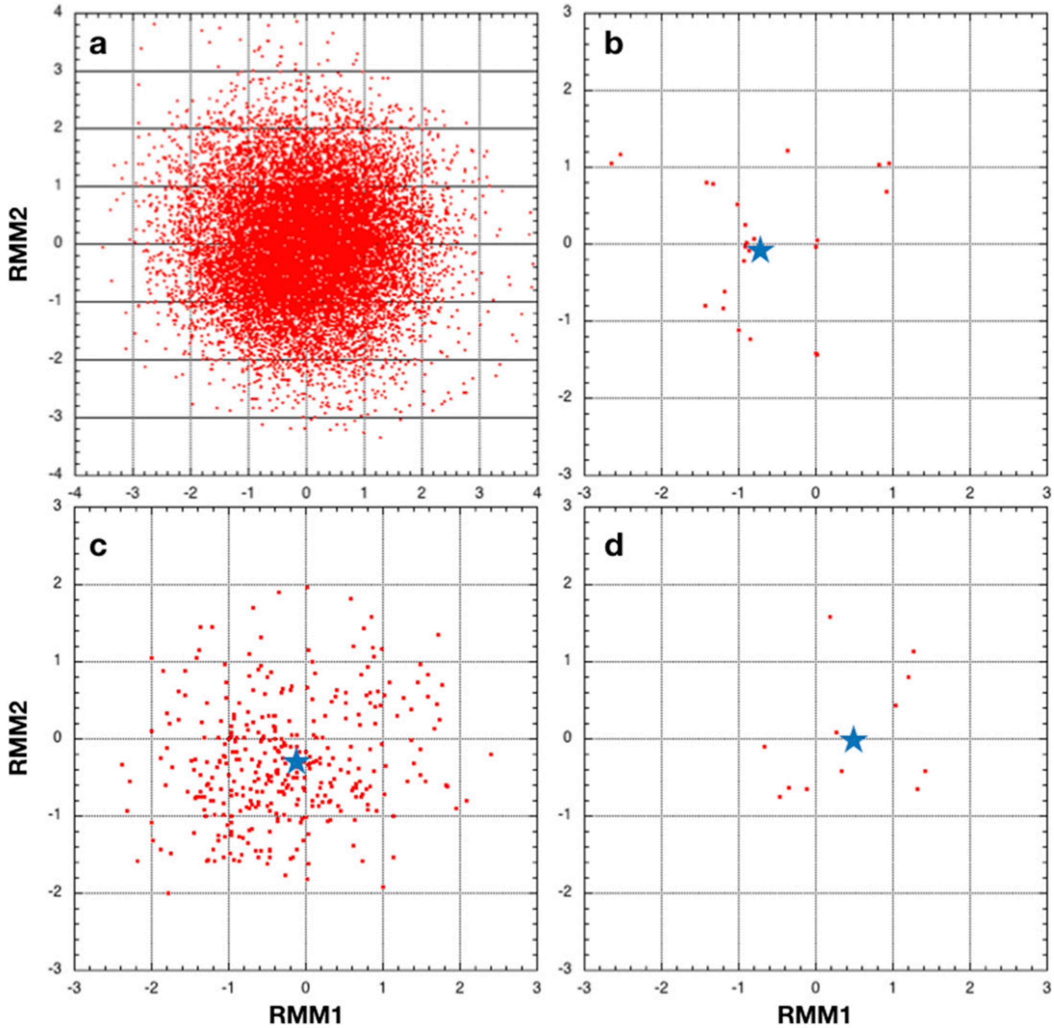

FIG. 2. Values of RMM1 and RMM2 (a) during the entire period of study (1974–2015), (b) for all RI events 160°W–180°, (c) for all RI events 80°–100°W, and (d) for all RI events 10°–30°W. The blue stars represent the means of each sample.

tested in the 10-predictor version of the Statistical Hurricane Intensity Prediction Scheme (SHIPS) Rapid Intensification Index (SHIPS-RII) operational in 2018. This scheme uses a linear discriminant analysis (Wilks 1995) to predict the likelihood that an individual tropical cyclone would intensify by various amounts of at least 30 kt for multiple lead times (Kaplan and DeMaria 2003; Kaplan et al. 2010, 2015). Because neither individual RMM components alone are significant RI predictors, a combination of the two must be used. Because the predictors used for the RII are consistently available only since 1995, only this part of the dataset is used. Figure 3 suggests that the MJO phase is associated with RI in different latitude bins, the difference between the tropical cyclone longitude and the phase $[\tan^{-1}(\mathrm{RMM1}/\mathrm{RMM2}) - \pi/2]$ could be an important predictor, with a negative correlation between the predictor and predictand. To test whether the amplitude is also important, this value is divided by the amplitude to create a second predictor. The two predictors were tested individually and together for both the Atlantic and east Pacific basins; results for the 30 kt $(24\,\mathrm{h})^{-1}$ and 55 kt $(48\,\mathrm{h})^{-1}$ thresholds are shown for brevity. The Brier skill score (BSS; Brier 1950) is calculated for each sample and for climatological forecasts, and the skill relative to the climatological forecasts $\{100 \times [1 - (\mathrm{BSS}_F/\mathrm{BSS}_C)]\}$, where F and C represent the forecast and climatology, respectively, is calculated. Cases impacted by land during the forecast period are removed from the sample.

Figure 5 shows the impact of the addition of these predictors on RI forecasts for the Atlantic and Pacific

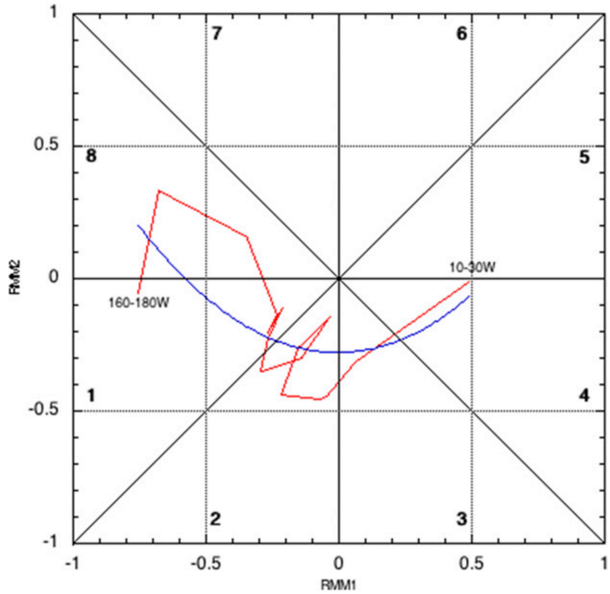

FIG. 3. Mean values of RMM1/RMM2 for all cases of RI within each 20° bin at 10° intervals (red line), and a polynomial fit to these values (blue line). The bold numbers represent the MJO phase.

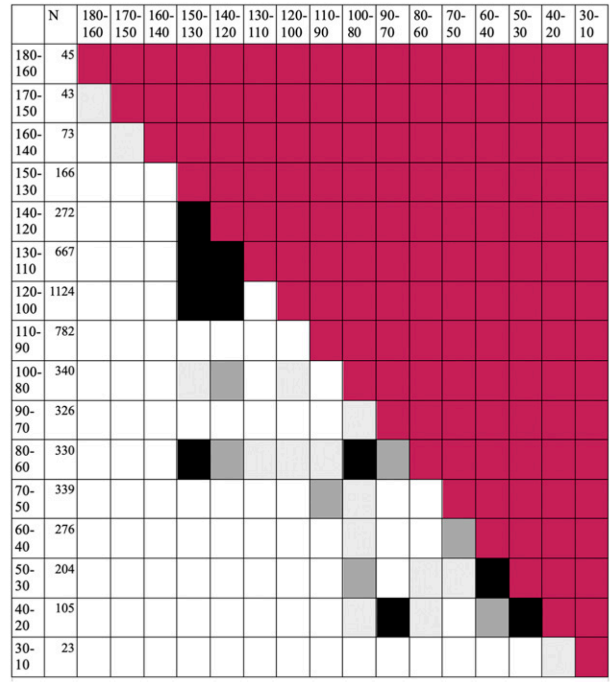

FIG. 4. Statistical significance between RMM1 and RMM2 values, tested individually, in all of the longitudinal bins. Black squares denote bins in which the mean of neither index is statistically different at 90%; dark gray shows bins in which the mean of neither index is different at 95%, and light gray shows bins in which the means of neither index are different at 99% significance. White squares denote bins in which one index shows a statistically significant difference at the 99% confidence level or higher. The number of RI events in each bin is shown.

basins separately. In both, the predictors only have a small, mixed impact on the BSSs. The absolute values of the correlations between the new and old predictors are all <0.15; this suggests that the new predictors do not duplicate information already available to the forecast scheme. One possible explanation for the lack of improvement is that the MJO is not related to RI itself, but instead to cyclogenesis, a necessary precursor to RI. Another possibility is that the large scatter (Fig. 2) in the RMM values limits the effectiveness of the new predictors. Because the MJO is likely to impact equatorial regions more than the midlatitudes, a sample limited to those cases in which the tropical cyclone is initially within 20° latitude of the equator (1962 cases) is also tested. In this more limited sample, the impacts are again small, but slightly more positive than in the full sample.

5. Conclusions

Klotzbach (2012), in their seminal study on the relationship between RI in the Atlantic and the MJO, found that RI is 4 times more likely during the active MJO phase than during the inactive phase. The current study extends this work to the central and east Pacific and tests whether the MJO may have predictive capability in current forecast schemes. All RI events in the part of the Western Hemisphere north of the equator along with the two commensurate RMM modes (Wheeler and Hendon 2004) are compiled from 1974 to 2015. The events are compiled into 20°-wide bins, and the mean values in each bin show that RI events and MJO events tend to move in tandem with each other from west to east across the hemisphere. Unlike in the Klotzbach (2012) study, the MJO is not generally in the most active convective phase in the region when RI occurs. Though the mean magnitudes are small, the differences between many bins are statistically significant. However, the addition of this information to statistical RI forecasting schemes does not significantly improve forecasts from SHIPS-RII, possibly because the MJO is not related to RI itself, but instead to cyclogenesis, a necessary precursor to RI, or due to the large scatter in the RMM values.

Though the results here show a relationship between the MJO and RI events in the hemisphere, they do not show improvements to current operational RI-prediction models. Despite this, other techniques, such as those based upon machine learning or other artificial intelligence algorithms, might be useful to pursue in the future.

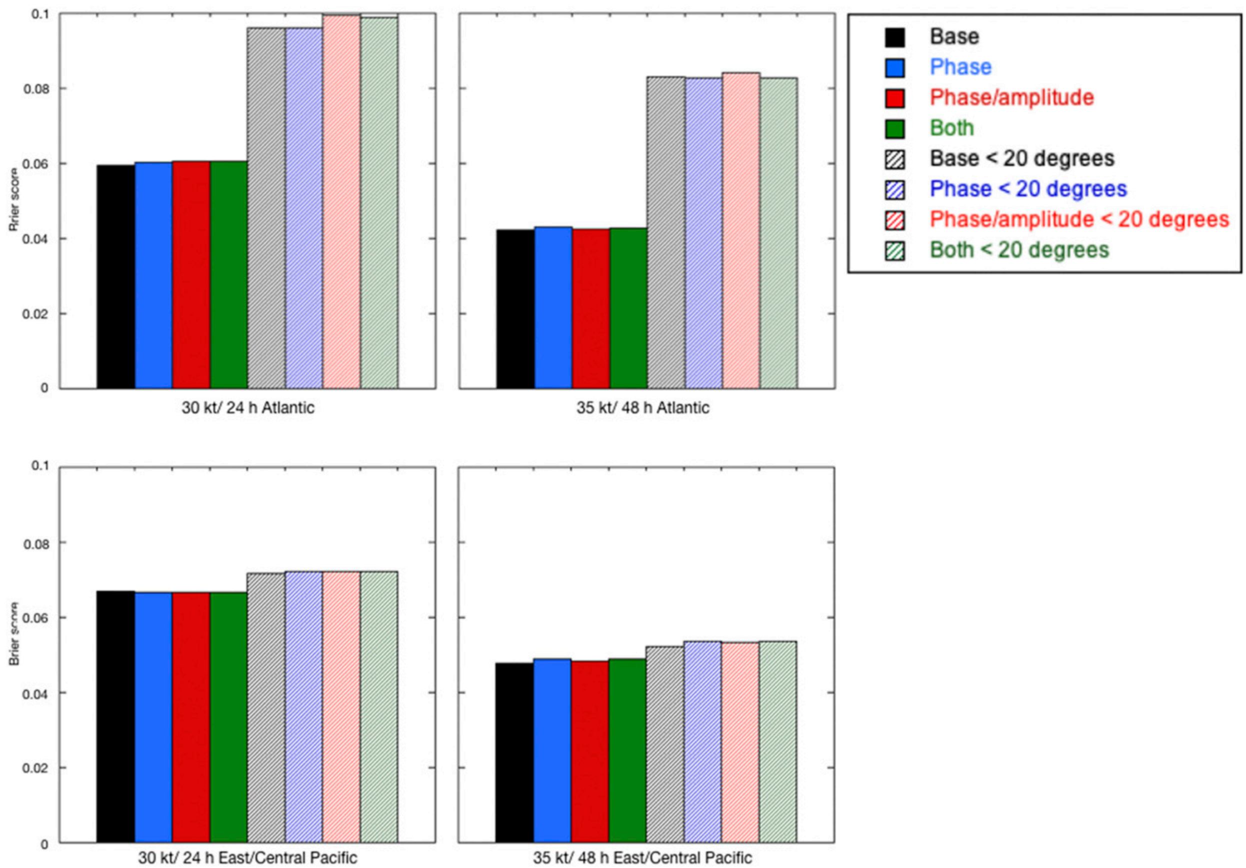

FIG. 5. Brier scores for RI forecasts for the (top) Atlantic basin and (bottom) east and central Pacific basins for two thresholds. Base represents forecasts using the most recent RI index model, phase represents forecasts using the base model and the difference between the TC and phase longitudes, phase/amplitude represents forecasts using the base model and the MJO phase and amplitude, and both shows forecasts using the base model and both new predictors. Hatched values are for cases in which the initial location is within 20° latitude of the equator.

Acknowledgments. The authors thank Mark DeMaria, Jason Dunion, and Gus Alaka for helpful comments on the research and manuscript drafts, and the three anonymous reviewers who helped to make this a clearer manuscript. Thanks also to Mike Jankulak for careful copyediting. The Australian Bureau of Meteorology provided the RMM data used in the study.

REFERENCES

Brier, G. W., 1950: Verification of forecasts expressed in terms of probability. *Mon. Wea. Rev.*, **78**, 1–3, https://doi.org/10.1175/1520-0493(1950)078<0001:VOFEIT>2.0.CO;2.

Camargo, S. J., M. C. Wheeler, and A. H. Sobel, 2009: Diagnosis of the MJO modulation of tropical cyclogenesis using an empirical index. *J. Atmos. Sci.*, **66**, 3061–3074, https://doi.org/10.1175/2009JAS3101.1.

Crosbie, E., and Y. Serra, 2014: Intraseasonal modulation of synoptic-scale disturbances and tropical cyclone genesis in the eastern North Pacific. *J. Climate*, **27**, 5724–5745, https://doi.org/10.1175/JCLI-D-13-00399.1.

Kaplan, J., and M. DeMaria, 2003: Large-scale characteristics of rapidly intensifying tropical cyclones in the North Atlantic basin. *Wea. Forecasting*, **18**, 1093–1108, https://doi.org/10.1175/1520-0434(2003)018<1093:LCORIT>2.0.CO;2.

——, ——, and J. A. Knaff, 2010: A revised tropical cyclone rapid intensification index for the Atlantic and eastern North Pacific basins. *Wea. Forecasting*, **25**, 220–241, https://doi.org/10.1175/2009WAF2222280.1.

——, and Coauthors, 2015: Evaluating environmental impacts on tropical cyclone rapid intensification predictability utilizing statistical models. *Wea. Forecasting*, **30**, 1374–1396, https://doi.org/10.1175/WAF-D-15-0032.1.

Kiladis, G. N., J. Dias, K. H. Straub, M. C. Wheeler, S. N. Tulich, K. Kikuchi, K. M. Weickmann, and M. J. Ventrice, 2014: A comparison of OLR and circulation based indices for tracking the MJO. *Mon. Wea. Rev.*, **142**, 1697–1715, https://doi.org/10.1175/MWR-D-13-00301.1.

Klotzbach, P. J., 2010: On the Madden–Julian Oscillation–Atlantic hurricane relationship. *J. Climate*, **23**, 282–293, https://doi.org/10.1175/2009JCLI2978.1.

——, 2012: El Niño–Southern Oscillation, the Madden–Julian oscillation and Atlantic basin tropical cyclone rapid intensification. *J. Geophys. Res.*, **117**, D14104, https://doi.org/10.1029/2012JD017714.

——, and E. C. J. Oliver, 2015: Modulation of Atlantic basin tropical cyclone activity by the Madden–Julian Oscillation (MJO) from 1905 to 2011. *J. Climate*, **28**, 204–217, https://doi.org/10.1175/JCLI-D-14-00509.1.

Landsea, C. W., and J. L. Franklin, 2013: Atlantic hurricane database uncertainty and presentation of a new database format. *Mon. Wea. Rev.*, **141**, 3576–3592, https://doi.org/10.1175/MWR-D-12-00254.1.

Leroy, A., and M. C. Wheeler, 2008: Statistical prediction of weekly tropical cyclone activity in the Southern Hemisphere. *Mon. Wea. Rev.*, **136**, 3637–3654, https://doi.org/10.1175/2008MWR2426.1.

Liebmann, B., H. H. Hendon, and J. D. Glick, 1994: The relationship between tropical cyclones of the western Pacific and Indian Oceans and the Madden–Julian oscillation. *J. Meteor. Soc. Japan*, **72**, 401–412, https://doi.org/10.2151/jmsj1965.72.3_401.

Madden, R. A., and P. R. Julian, 1972: Description of global-scale circulation cells in the Tropics with a 40–50 day period. *J. Atmos. Sci.*, **29**, 1109–1123, https://doi.org/10.1175/1520-0469(1972)029<1109:DOGSCC>2.0.CO;2.

Slade, S. A., and E. D. Maloney, 2013: An intraseasonal prediction model of Atlantic and east Pacific tropical cyclone genesis. *Mon. Wea. Rev.*, **141**, 1925–1942, https://doi.org/10.1175/MWR-D-12-00268.1.

Ventrice, M. J., C. D. Thorncroft, and P. E. Roundy, 2011: The Madden–Julian oscillation's influence on African easterly waves and downstream tropical cyclogenesis. *Mon. Wea. Rev.*, **139**, 2704–2722, https://doi.org/10.1175/MWR-D-10-05028.1.

Wheeler, M., and H. H. Hendon, 2004: An all-season real-time multivariate MJO index: Development of an index for monitoring and prediction. *Mon. Wea. Rev.*, **132**, 1917–1932, https://doi.org/10.1175/1520-0493(2004)132<1917:AARMMI>2.0.CO;2.

Wilks, D. S., 1995: *Statistical Methods in the Atmospheric Sciences: An Introduction*. International Geophysics Series, Vol. 59, Elsevier, 467 pp.

Zhao, C., and T. Li, 2019: Basin dependence of the MJO modulating tropical cyclone genesis. *Climate Dyn.*, **52**, 6081–6096, https://doi.org/10.1007/s00382-018-4502-y.